

Radio-frequency magnetometry in atomic vapor using Nonlinear magnetoelectric effect

Soumya R. Mishra^{1,*}, Sushree S. Sahoo^{1,2}, G.Rajalakshmi², Ashok K. Mohapatra^{1,#}

¹National Institute of Science Education and Research Bhubaneswar, Jatni 752050, HBNI, India

²TIFR Centre for Interdisciplinary Sciences, Tata Institute of Fundamental Research, Hyderabad 500046, India

*soumya.ranjan.mishra@niser.ac.in #a.mohapatra@niser.ac.in

Abstract

We present the nonlinear magnetoelectric (ME) effect in atomic vapor which refers to the coupling between input optical electric field and radio-frequency (rf) magnetic fields resulting in the generation of new optical fields. We do the density matrix calculations for theoretical modeling of the ME effect and obtain various experimental results which validate the effect in atomic vapor. This ME effect paves the way for rf-magnetometry, and we could achieve the best rf-field sensitivity of 70 fT/ $\sqrt{\text{Hz}}$ at 1 kHz to 7.5 fT/ $\sqrt{\text{Hz}}$ at 3 MHz in an unshielded environment for zero biasing magnetic fields. The proposed magnetometer has a high dynamic range up to 10^{12} and a 6 dB bandwidth of 450 kHz with arbitrary frequency resolution.

Introduction

The ME effect in a medium refers to the parametric interaction of input optical electric and rf-magnetic fields. The coupling inside the medium results in the electric polarization induced by magnetic fields whereas magnetization is induced by electric fields and expressed as,

$$P_E(t) = \chi_E^{(1)} E(t) + \chi_E^{(2)} E(t)^2 + \chi_{EEM}^{(2)} E(t)B(t) + \chi_E^{(3)} E(t)^3 + \chi_{EEMM}^{(3)} E(t)B(t)^2 + \dots \quad (1)$$

In the above expression, the third and fifth nonlinear terms are responsible for the nonlinear magnetoelectric effects in our system corresponding to three-wave and four-wave mixing processes. Previously ME effects have been reported in various solid-state systems like some heterostructures because of their diverse applications in the fabrication of magnetic sensors and memories^{1,2}. But in our work, we demonstrate this nonlinear ME effect in an atomic vapor medium and its practical usefulness in radio-frequency (rf) magnetic field sensing³. Usually in atomic vapor, previous works on rf-magnetometry have been demonstrated with the polarimetry technique⁴⁻⁶. Whereas in our case by using the nonlinear ME effect we perform the rf-magnetometry in an unshielded environment for zero biasing fields and achieve the best rf-field sensitivity of 70 fT/ $\sqrt{\text{Hz}}$ at 1 kHz to 7.5 fT/ $\sqrt{\text{Hz}}$ at 3 MHz.

Theory

Our system consists of a four-level atomic system with three degenerate ground states of $F = 1$ and a single excited state of $F' = 0$. We put a dc magnetic field (B_0) in the propagation direction to split the Zeeman sublevels of the ground state and a transverse rf-magnetic field (ω_{rf}) coupling the ground states, builds the coherence between those sublevels as shown in Fig-1. An input optical field (ω_p) coupling between one of the ground states to the excited state, interacts with rf-induced coherence to generate new optical frequencies $\omega_p \pm \omega_{\text{rf}}$ and $\omega_p \pm 2\omega_{\text{rf}}$ involving a three-wave and four-wave mixing processes.

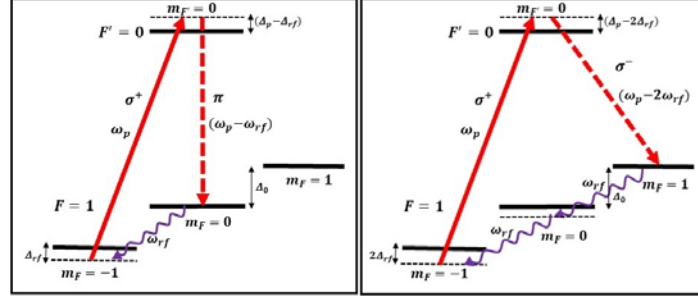


Fig 1: Schematics of the Mixing process in energy level diagram of ^{87}Rb .

The time-independent Hamiltonian of the four-level system in presence of a dc and rf magnetic field is given as,

$$\hat{H}' = -\hbar \begin{pmatrix} -\Delta_{rf} & \Omega_{rf} & 0 & \Omega_p^* \\ \Omega_{rf}^* & 0 & \Omega_{rf} & 0 \\ 0 & \Omega_{rf}^* & \Delta_{rf} & 0 \\ \Omega_p & 0 & 0 & -(\Delta_p + \Delta_{rf}) \end{pmatrix} \quad (2)$$

Where Ω_p and Ω_{rf} are rabi frequencies of input optical and rf magnetic fields respectively and Δ_p and Δ_{rf} are their corresponding detunings. To model the system we solve Bloch's equation given as,

$$\frac{d\rho}{dt} = \frac{-i}{\hbar} [\hat{H}', \rho] + \hat{L}_D \quad (3)$$

For a weak rf field approximation, the analytical solutions for coherence terms ρ_{42} and ρ_{43} are expressed as,

$$\rho_{42} = \frac{-\Omega_p \Omega_{rf}}{\Delta_p (2\Delta_{rf} + i\gamma)} \quad \rho_{43} = \frac{\Omega_p \Omega_{rf}^2}{\Delta_p (\Delta_{rf} + i\gamma) (2\Delta_{rf} + i\gamma)} \quad (4)$$

From the above expressions, we determine the coherence term $\rho_{42}(\rho_{43})$ depends linearly(quadratically) on rf field amplitude(Ω_{rf}).

Experimental Methods and Results

A vapor cell containing Rubidium atoms at around 80°C is kept inside a μ -metal shielding to discard any stray magnetic fields. Three pairs of Helmholtz coils wrapped around the cell to produce a uniform rf magnetic field inside the cell as shown in Fig-2. A part of the initial beam after passing through the AOM combination gets frequency shifted and will be treated as a local oscillator. The first waveplate is used to choose any polarization of input light either circular or linear polarizations whereas the second one is used to revert back to the initial polarization.

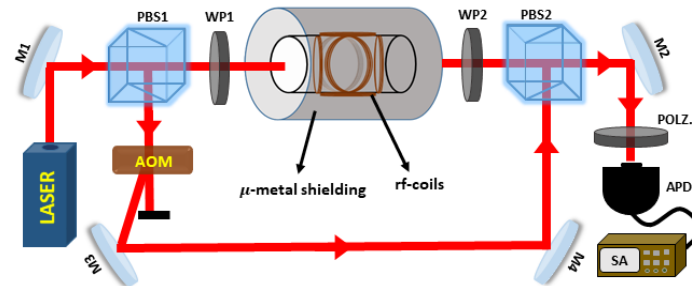


Fig 2: Schematic of Experimental Set-up

For a circularly polarized input pump beam the generated optical fields will be linear and orthogonal circular polarized. Interference beats of generated optical fields and local oscillator after passing the second PBS observed through spectrum analyzer via photodetector. We record the beat amplitudes with varying input parameters and obtained various experimental results discussed below.

First, we observe the δ and 2δ beat amplitudes vary with rf field frequencies and follow a resonance behavior. For a particular rf frequency where it matches the frequency of Zeeman splitting, the mixing process is more efficient for which the beat amplitudes get maximized as shown in Fig-3.

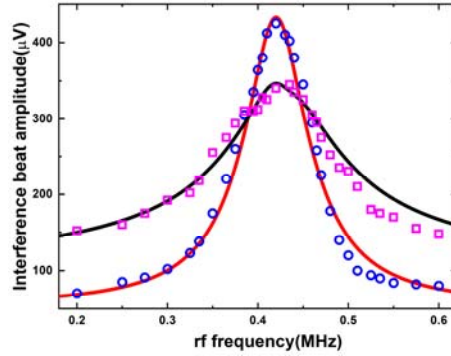


Fig 3: Depiction of beat amplitude variation with rf field frequencies

At weak rf field approximation, the experimental data of three-wave and four-wave mixing processes (magenta squares and blue circles) matches well with the theoretical plot (black and red solid lines) and the rf resonance frequency is found to be 425 kHz. We also demonstrate the dependence of beat amplitudes on rf magnetic field intensity by varying the current of Helmholtz coils as plotted below.

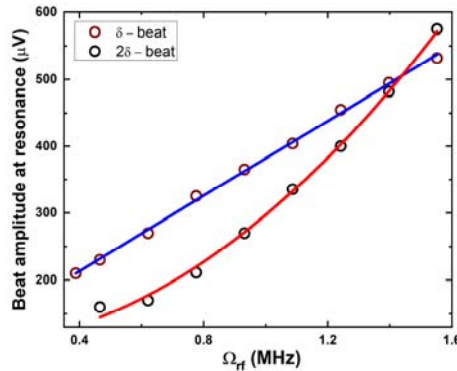


Fig 4: Schematic of dependence of beat amplitude on rf field Rabi frequency

Theoretical prediction of Eq. 4 indicates the dependence of coherence term $\rho_{42}(\rho_{43})$ on rf field amplitude (Ω_{rf}) linearly (quadratically) matches with the experimental plot as shown in Fig-4, which validates the ME effect. In the above figure black (brown) circles represent experimental data points whereas the red (blue) solid lines are their respective theoretical fitting.

rf-Magnetometry

To calculate rf field sensitivity we record the beat signal and corresponding noise floor per unit bandwidth for frequencies ranging from 1kHz to 3MHz, from where we then get the Signal-to-Noise Ratio (SNR). Hence the rf magnetic field sensitivity is calculated using the expression,

$$\delta B = \frac{B_{rf}}{SNR} \quad (5)$$

We experimentally measure the magnetic field sensitivity at various rf frequencies (1kHz-3MHz) and zero bias field in an unshielded environment, presented in Fig-5.

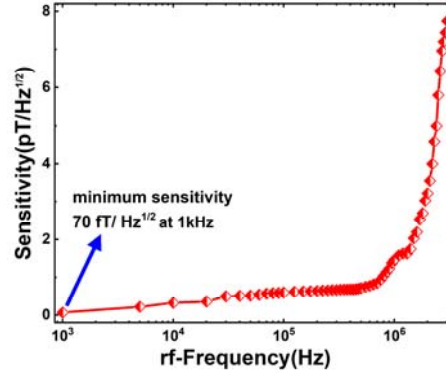


Fig 5: Schematic of rf-magnetic field sensitivity with rf frequencies

We could achieve the best sensitivity of 70 fT/ $\sqrt{\text{Hz}}$ at 1 kHz to 7.5 fT/ $\sqrt{\text{Hz}}$ at 3 MHz in an unshielded environment with a frequency resolution limited to the measurement device. The dynamic range of our system is calculated to be up to 10^{12} and a 6 dB bandwidth of 450 kHz with arbitrary frequency resolution.

Conclusion

we can study various nonlinear magneto-optical effects involving the coupling of electric and rf magnetic fields in an atomic vapor medium and it could be useful for rf magnetometry due to some interesting features like arbitrary frequency resolution, high dynamic range, and large bandwidth.

Acknowledgment

I would acknowledge the financial support from the Department of Atomic Energy, Govt. of India, NISER Bhubaneswar, and TIFR Hyderabad.

References

1. Sushree S. Sahoo, Soumya R. Mishra, G. Rajalakshmi, and Ashok K. Mohapatra, *Phys. Rev. A* **105**, 063509(2022).
2. L Y Fetisov et al *J. Phys. D: Appl. Phys.* **51** 154003 (2018).
3. D. A. Filippov, V. M. Laletin and T. O. Firsova, *Phys. Solid State* **56**, 980–984 (2014).
4. I. M. Savukov, S. J. Seltzer, M. V. Romalis, and K. L. Sauer, *Phys. Rev. Lett.* **95**, 063004 (2005).
5. D. Budker and M. Romalis, *Nat. Phys.* **3**, 227–234 (2007).
6. W. Chalupczak, R. M. Godun, S. Pustelny, and W. Gawlik, *Appl. Phys. Lett.* **100**, 242401 (2012).